Deoxyribozymes with 2'–5' RNA Ligase Activity

Amber Flynn-Charlebois, Yangming Wang, Tracey K. Prior, Imran Rashid, Kelly A. Hoadley, Rebecca L. Coppins, Amanda C. Wolf, and Scott K. Silverman*

Contribution from the Department of Chemistry, University of Illinois at Urbana-Champaign, 600 S. Mathews Ave., Urbana, Illinois 61801

Figures in this Supporting information are prefixed by the letter X (e.g., Figure X1) to distinguish them from the manuscript Figures. All references cited by number are from the manuscript. See the manuscript's Experimental Section for details.

Determining the 3'–5' or 2'–5' linkage for ligated RNA products from individual deoxyribozymes

The ligated RNA products from the 9A12, 9A5, 9A6, and 9A2 deoxyribozymes were assayed using the methods of Figure 3. The results in Figure X1 show that the RNA product from each of the four deoxyribozymes is unambiguously linked 2'–5' (>95%).

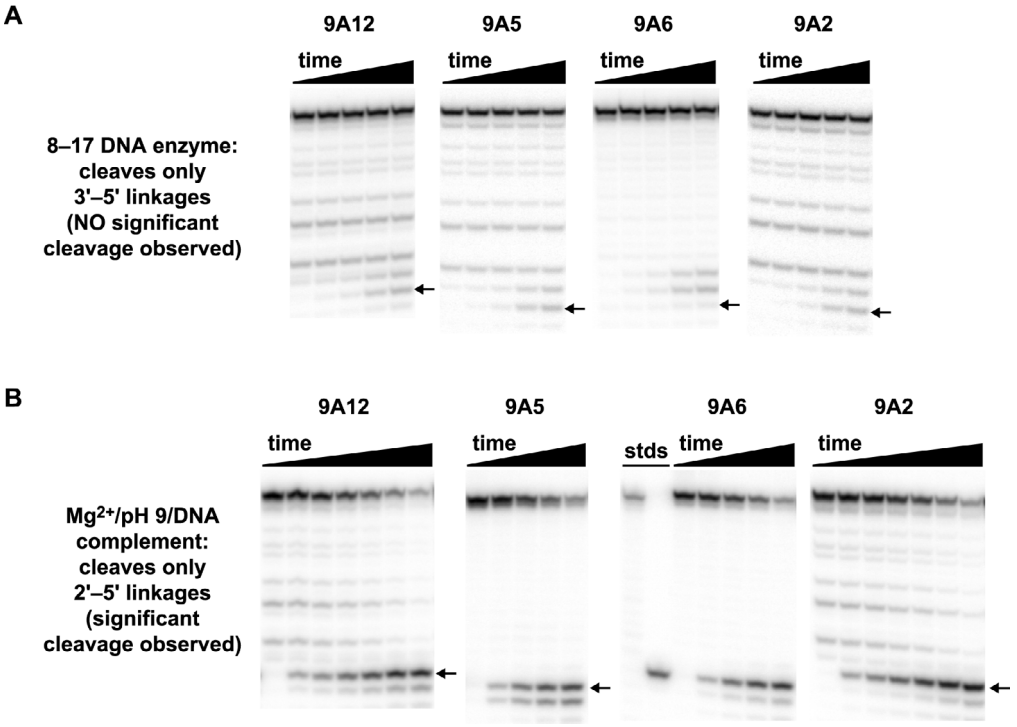

Figure X1. Determining the ligation junctions from the new DNA enzymes 9A12, 9A5, 9A6, and 9A2, using the two assays of Figure 3. (A) The 8–17 assay that cleaves only 3'–5' linked RNA. Timepoints for all, 0-7 h. (B) The Mg^{2+}/pH 9 assay that cleaves only 2'–5' linked RNA. Timepoints: 9A12 and 9A2, 0-33 h; 9A5 and 9A6, 0-24 h. For all panels, the small arrow indicates the location of the cleavage standard, in those cases where that standard is in a nonadjacent location on the gel image. In panel A, note that no specific product band is formed, only a small amount of background cleavage/degradation (<5%). This contrasts sharply with the complete cleavage of the 3'–5' standard RNA under the same conditions as shown in Figure 3A. In panel B, the timecourse of cleavage is quantitatively similar to that observed with the 2'–5' linked standard RNA under the same conditions (Figure 3B), with hydrolysis $t_{1/2}$ ~11 h (ref. 19).

Alkaline hydrolysis of the ligated RNA products to demonstrate their linearity

As a further check on the ligation junction of the RNA products created by the four new deoxyribozymes, we subjected the same ligated products that were assayed in Figure X6 to partial alkaline hydrolysis (Figure X2). From each ligated product, a continuous ladder of bands was observed under conditions in which each RNA molecule is hydrolyzed at most once ("single-hit conditions"). This indicates that each ligated product is linear. The assay does not distinguish between 3'–5' and 2'–5' linked RNA. However, it does confirm that each RNA is not branched in any unexpected way; e.g., by attack of an internal 2'-hydroxyl from the right-hand substrate on the cyclic phosphate, rather than attack of the 5'-terminal hydroxyl group. If this were the case, then the alkaline hydrolysis ladder would be interrupted by a gap at the branch point, due to the missing 2'-hydroxyl at that position. We have obtained branched RNA from other selections (Y.W., R.L.C., and S.K.S., unpublished results), and in such instances, gaps in the alkaline hydrolysis ladder are clearly observed.

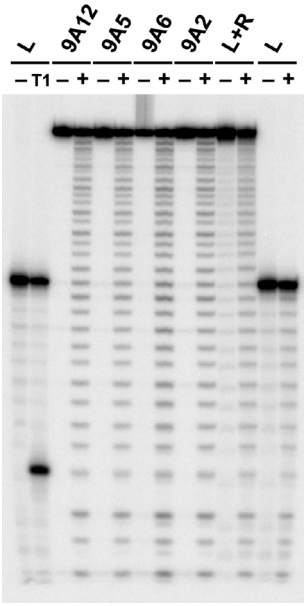

Figure X2. Partial alkaline hydrolysis of the ligated RNA products from the new deoxyribozymes. The ligated products from the intermolecular reaction of Figure 4A were incubated in 50 mM $NaHCO_3$, pH 9.0 for 10 min at 90 °C and analyzed by 20% PAGE. Standards were the left-hand RNA substrate L terminating in a 2',3'-cyclic phosphate or the 3'–5' linked L+R. Above each line, – indicates no incubation; + indicates partial alkaline hydrolysis; and T1 indicates incubation with ribonuclease T1 (Ambion), which cleaves after the only guanosine residue in the L substrate and thus allows firm assignments of the bands in the ladders. See Figure 7A for the substrate sequences ("original"); the 5'-GGA was not present in the substrates analyzed here.

Dependence of ligation on phosphorylation state of RNA substrate termini

To provide evidence that the new deoxyribozymes ligate the 2',3'-cyclic phosphate and 5'-hydroxyl of the RNA substrates, we tested the dependence of ligation on the presence of the appropriate functional groups on the ends of the RNA substrates (Figure X3). The 2',3'-cyclic phosphate was replaced with a 2',3'-diol; the 5'-hydroxyl was changed to a 5'-monophosphate; or both changes were made simultaneously. The assays confirm that both the 2',3'-cyclic phosphate and 5'-hydroxyl are strictly required for ligation for all four deoxyribozymes. While this experiment does not *prove* that a phosphodiester bond is formed by reaction of the 5'-hydroxyl with the 2',3'-cyclic phosphate, it is a

necessary requirement for that to be the case. The assays described in Figure 3 to distinguish 3'–5' and 2'–5' linkages confirm that a phosphodiester bond is indeed formed in the ligation reactions.

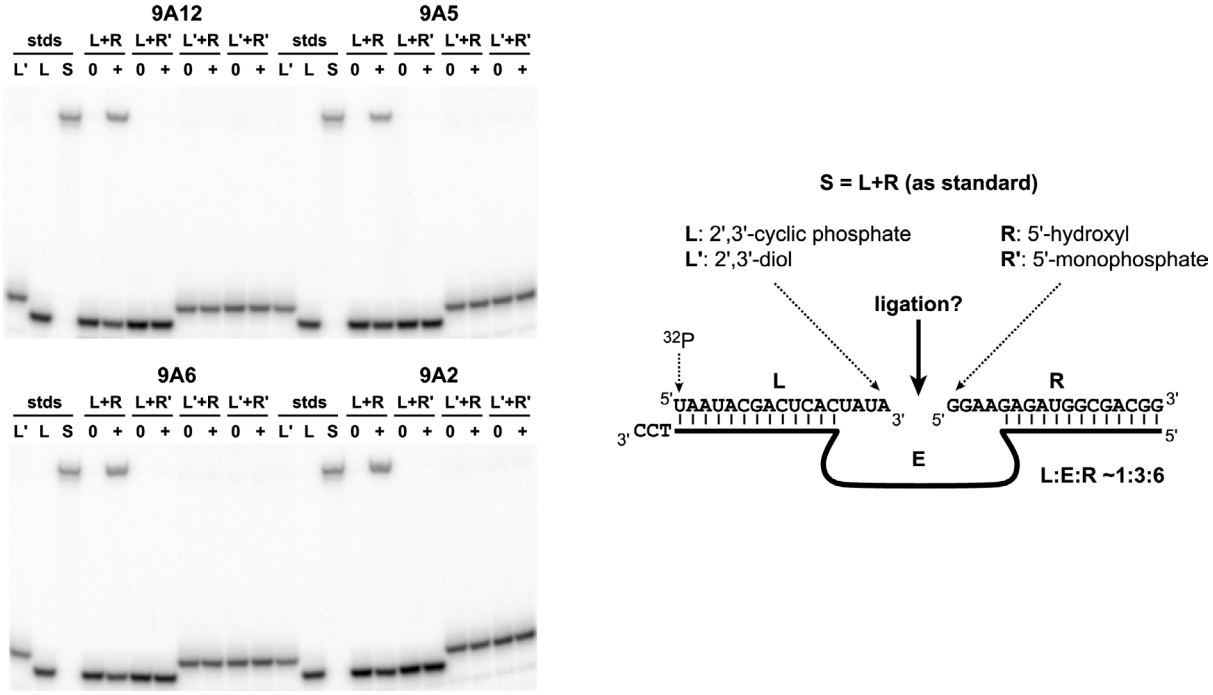

Figure X3. Testing the dependence of ligation on the terminal functional groups of the two RNA substrates. L and R denote RNA substrates with the termini used during selection (2',3'-cyclic phosphate and 5'-hydroxyl), whereas L' and R' denote the "wrong" termini. On the gels, "0" indicates a timepoint taken immediately after mixing, and "+" indicates a suitable reaction time (12 h for 9A12, 9A6, and 9A2; 4 h for 9A5).

Multiple turnover assays

The standard RNA ligation assays (Figure 4) were conducted under single-turnover conditions, with L:E:R ratio typically 1:3:6 (1.5 μM E) and 5'-^{32}P-radiolabeled L as the limiting reagent. To assay for multiple turnover, ligation reactions were performed with L:E ratios of 4:1 to 40:1 (1.2 to 12 μM E) and several-fold excess of R relative to L in each case. Under these conditions, if multiple turnover occurs, then the amount of ligated product should be greater than the theoretical amount calculated from the L:E ratio and assuming only one turnover per E molecule. However, in no tested case was evidence for multiple turnover found. The simplest explanation is that multiple turnover does not occur because the DNA enzyme binds the ligated products (L+R) more tightly than it does the reactant substrates (product inhibition). Multiple turnover was not detected even when E had relatively short substrate binding arms. Short binding arms were predicted to favor turnover, by having the enzyme bind relatively weakly to the product as well as the ligation substrates.

Temperature dependence of ligation rate and yield

Ligation experiments were performed at 10 °C and pH 7.5, to check if the rates and/or yields improved at lower temperature. This was prompted by a recent study that reported higher ligation yields for the hammerhead ribozyme at lower temperature (ref. 20). Ligation experiments at 45 °C were also examined. The results are shown in Figure X4 and indicate that either decreasing or increasing the reaction temperature does not assist the ligation by the new deoxyribozymes.

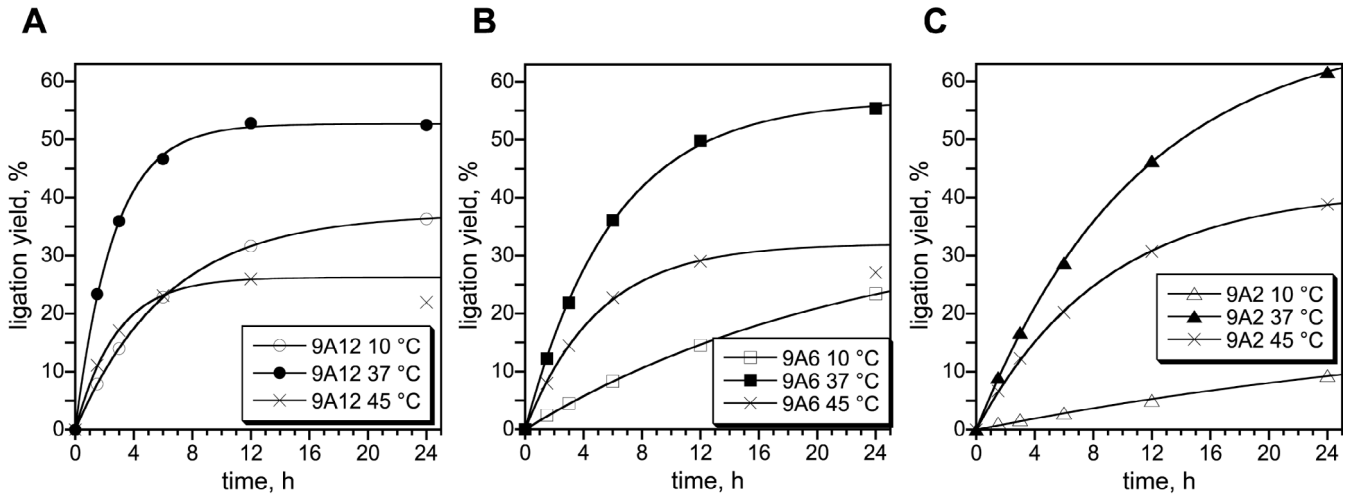

Figure X4. Ligation assays for the new deoxyribozymes at 10, 37, and 45 °C (all at pH 7.5). The procedure was the same as for the data reported in Figure 4C. (A) Data for 9A12. Values of k_{obs} (h^{-1}): 10 °C, 0.16; 37 °C, 0.38; 45 °C, 0.36. The 24-h point at 45 °C was not fit because the gel image clearly shows some degradation (data not shown). (B) Data for 9A6. Values of k_{obs} (h^{-1}): 10 °C, 0.043; 37 °C, 0.17; 45 °C, 0.20. The 24-h point at 45 °C was not fit because the gel image clearly shows some degradation (data not shown). (C) Data for 9A2. Values of k_{obs} (h^{-1}): 10 °C, 0.025; 37 °C, 0.09; 45 °C, 0.11. Analogous experiments were performed for 9A5 at 10 °C (0-24 h timepoints) and 37 and 45 °C (0-90 min timepoints; data not shown). The fits were as follows: 10 °C, k_{obs} = 0.037 h^{-1} and 16% yield at t = ∞; 37 °C, k_{obs} = 0.90 h^{-1} and 31% yield at t = ∞; 45 °C, k_{obs} = 1.8 h^{-1} and 23% yield at t = ∞.

Assays with control splints at 37 °C and pH 9.0

The control ligation assays with short complementary DNA splints were performed at 37 °C and 50 mM CHES, pH 9.0 (Figure X5), similar to those in Figure 6 at pH 7.5. The same dependence on number of nucleotides inserted into the splint was observed. If k_{obs} = 0.000032 min^{-1} is taken as the background rate (the value for the T_4 splint from Figure X5), then the calculated rate enhancements for 9A5 and 9A2 are 5600 and 720, respectively. These values are slightly higher than the enhancements calculated at pH 7.5 by comparison to k_{obs} for the T4 splint under those conditions (see manuscript).

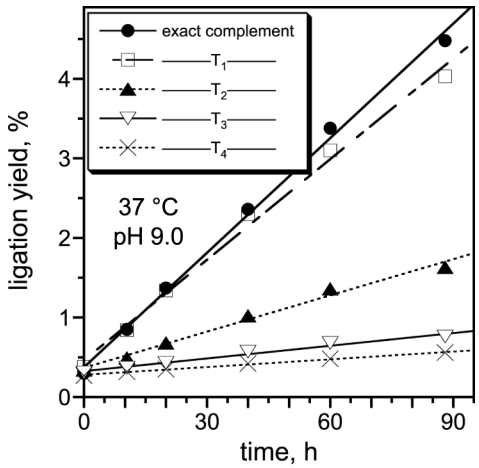

Figure X5. Control ligation assays with short complementary DNA splints at 37 °C and 50 mM CHES, pH 9.0. Experiments were performed as in Figure 6. The detection limit for this experiment was ~0.3%. The slopes of the linear fits were (n=0 to 4 inserted T nucleotides, top to bottom, min^{-1}) 0.00048, 0.00042, 0.00015, 0.000053, and 0.000032.

Assaying RNA substrate sequence dependence of ligation: modifications directly at the ligation junction

We assayed the abilities of the four new deoxyribozymes to ligate substrates with various nucleotides directly at the ligation junction (Figures X6 and X7). The ligation junction is generically denoted X↓Y; for example, A↓G is the particular junction formed in the selection procedure. The four possible right-hand RNA substrates (where the 5'-most nucleotide is G in the selection procedure) were obtained by solid-phase synthesis at Dharmacon. The four left-hand substrates, each bearing a 2',3'-cyclic phosphate, were obtained in two ways. Those with an A or a G at the 3'-end were obtained by using a 10–23 deoxyribozyme as described in the manuscript; the 10–23 deoxyribozyme cleaves only after purines. Those substrates with a 3'-terminal A, U, or C were obtained by in vitro T7 RNA polymerase transcription from a PCR-generated DNA template that encodes the sequence of interest terminating with a self-cleaving hammerhead ribozyme. To enable in vitro transcription of the latter RNAs, three extra nucleotides GGA were included at the 5'-end, so these left-hand substrates are three nucleotides longer than those prepared by solid-phase synthesis (see "original" sequence in Figure 7A). Note that the left-hand substrate with a 3'-terminal A was prepared and tested in both formats.

The results in Figure X6 show that the 9A12, 9A6, and 9A5 deoxyribozymes are intolerant of changes on either side of the ligation junction; that is, they strictly require a A↓G junction. In contrast, the 9A2 deoxyribozyme is moderately tolerant of any nucleotide on the left side. That is, its requirement is N↓G, although pyrimidines are less well tolerated at the N position than are purines by several-fold in terms of yield.

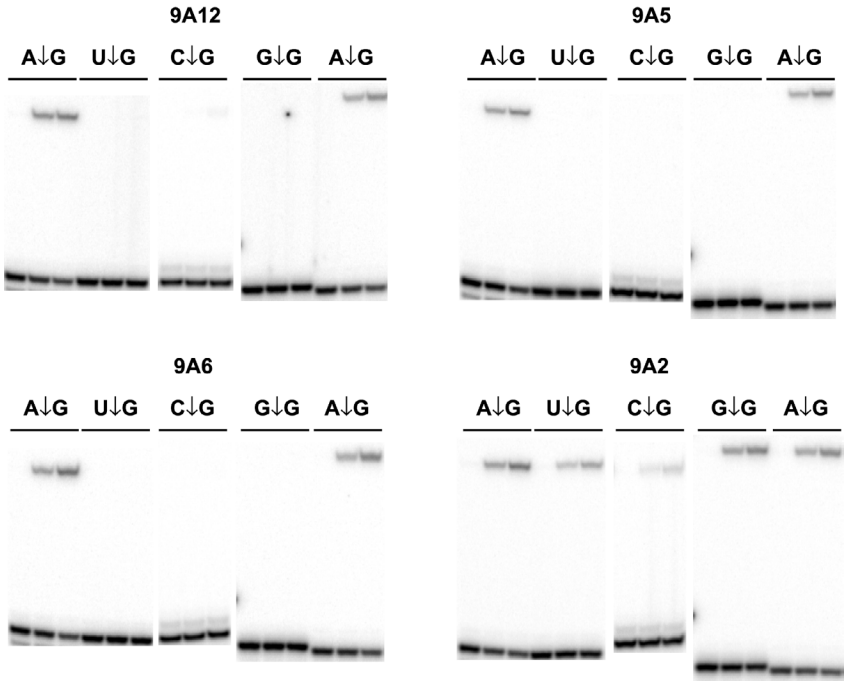

Figure X6. Testing the tolerance of the new deoxyribozymes for various nucleotides directly on the left side of the ligation junction. In each panel, the three tests on the left used left-hand substrate RNA prepared by hammerhead-terminated transcription, and the two tests on the right used left-hand substrate RNA prepared by 10–23 deoxyribozyme cleavage of a precursor RNA . Timepoints: 9A12 0, 3, and 12 h; 9A5 0, 1, and 6 h; 9A6 0, 3, and 12 h; 9A2 0, 6 and 14 h. For 9A2, the % ligated at 14 h was (left to right) 32, 12, 4.7, 21, and 31.

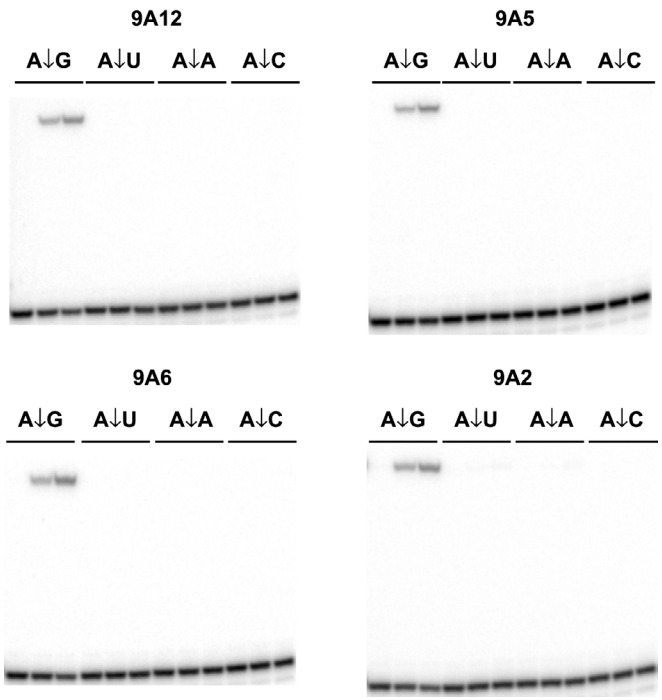

Figure X7. Testing the tolerance of the new deoxyribozymes for various nucleotides directly on the right side of the ligation junction. Timepoints as in Figure X6.

Assaying RNA substrate sequence dependence of ligation: modifications surrounding the ligation junction

Because the selection strategy used four-nucleotide single-strand overhangs on either side of the ligation junction, we were hopeful that some of these nucleotides of the RNA substrates could be varied while still retaining ligation activity with the selected deoxyribozymes. This was tested with a panel of substrate RNAs in which each of the six positions in the overhangs *not* immediately at the ligation site were changed to the other pyrimidine or purine (i.e, transitions; U→C, A→G, etc.; Figure X8). This provides a systematic overview of the tolerance of these regions to nucleotide changes. (It is important to note that the deoxyribozymes may in fact use one or more nucleotides from their enzyme region to base-pair with these nucleotides, as indicated in the manuscript.) Each modified left-hand RNA substrate was prepared by in vitro T7 RNA polymerase transcription from a PCR-generated DNA templates that encodes the sequence of interest terminating with a self-cleaving hammerhead ribozyme. For the RNA with 3'-terminus ...UACA, the rate of hammerhead processing was so low as to be preparatively useless, so the uncleaved transcript (still containing the hammerhead) was cleaved in trans with an 8–17 deoxyribozyme. Each modified right-hand RNA substrate was prepared by in vitro transcription from a double-stranded DNA template obtained by annealing two oligonucleotides prepared by solid-phase synthesis.

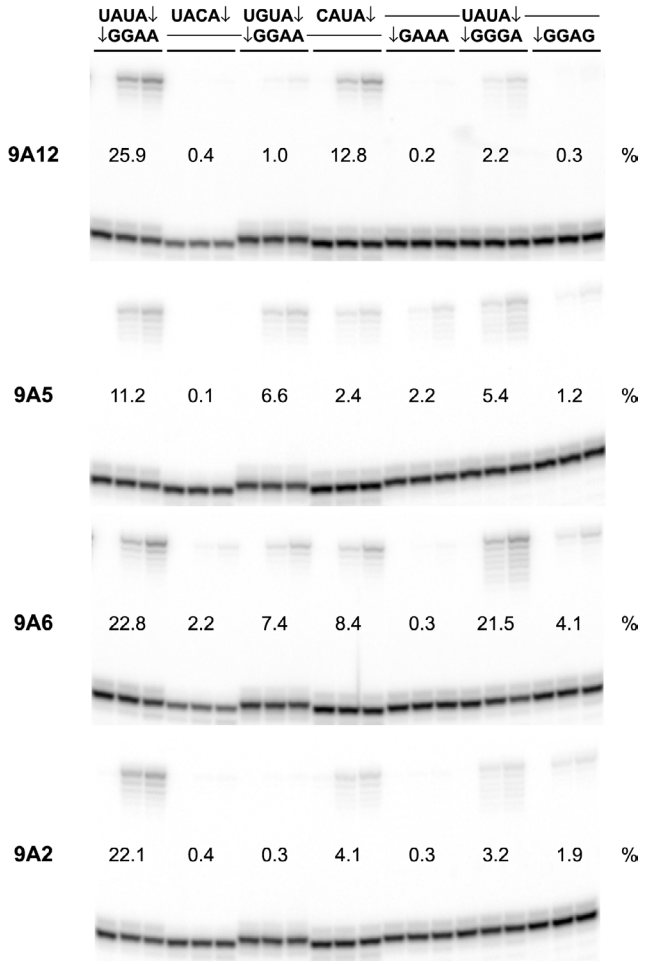

Figure X8. Testing the tolerance of the new deoxyribozymes for various nucleotides in the regions surrounding the ligation site. In each panel, test #1 (counting left to right) used substrate RNAs corresponding to the original sequences used during selection (Figure 7A); tests #2-4 used substrate RNAs differing at one nucleotide in the left-hand substrate; and tests #5-7 used substrate RNAs differing at one nucleotide in the right-hand substrate. The eight nucleotides (four on each side) surrounding the ligation junction are shown above each set of lanes. Timepoints: 9A12 0, 3, and 12 h; 9A5 0, 1, and 8 h; 9A6 0, 3, and 12 h; 9A2 0, 8 and 14 h. The % ligated at the final timepoint is shown within each gel. The faint lower bands for each ligated product are apparently due to slight decomposition during dephosphorylation of the transcribed right-hand substrate oligonucleotides; other samples from different experiments did not show this effect, which is apparently due to an impurity in a specific sample of alkaline phosphatase. Note that even the "parent" (UAUA↓GGAA) ligations in the first test of each panel (which used right-hand substrate that was transcribed then dephosphorylated) here show the lower bands, whereas such bands are not evident in the ligation experiments shown in the other figures. The faint lower bands are *not* due to a ragged 3'-end from transcription, which would instead give faint bands above (rather than below) the most intense band for ligated product.

Ligations to form the P4-P6 domain of the *Tetrahymena* group I intron RNA

The 9A6 deoxyribozyme (denoted E) was used to prepare P4-P6 by ligation. The two RNA substrates to be joined were denoted $L^{P4\text{-}P6}$ (nucleotides 102 through 233 of the P4-P6 sequence, ref. 22) and $R^{P4\text{-}P6}$ (P4-P6 nucleotides 234 through 261). $L^{P4\text{-}P6}$ with a 3'-terminal 2',3'-cyclic phosphate was prepared by in vitro T7 RNA polymerase transcription from a PCR-derived DNA template that additionally encodes the HDV ribozyme sequence at its 3' end. $R^{P4\text{-}P6}$ was prepared by transcription from annealed DNA oligonucleotides and subsequently dephosphorylated with CIP before ligation. The ligation junction between nucleotides A233 and G234 is adjacent to the L6b loop of P4-P6, as shown in manuscript Figure 3B. Because the 9A6 deoxyribozyme has some substrate sequence requirements at the four nucleotides on either side of the ligation junction (see Figures X6–X8), several nucleotide changes relative to wild-type P4-P6 were made in the substrates $L^{P4\text{-}P6}$ and $R^{P4\text{-}P6}$. Specifically, the four boldface nucleotide changes of Figure 9A (i.e., C232U, A235G, U236A, and C237A) were made. In addition, because 9A6 provided optimal yield with the RNA sequence UAUA immediately 5' of the ligation junction, the mutation A230U was also made. Note that the test substrates of Figure 7A ("new" sequences) correspond to the nucleotides surrounding the P4-P6 A233↓G234 ligation junction, with incorporation of the nucleotide changes just described. The substrate binding arms of the deoxyribozyme E were chosen to complement the RNA substrate sequences with Watson-Crick base pairs.

We expected the A230U mutation to disrupt base pairing in the stem above L6b by creating a U-U mismatch (see Figure X10A below). Therefore, we performed *two* ligation reactions to prepare P4-P6: one with $L^{P4\text{-}P6}$ containing both the A230U and C232U mutations, and one with $L^{P4\text{-}P6}$ containing only the C232U mutation. The latter substitution replaces a C-G base pair with a U•G wobble pair in P4-P6 and thus should be more structurally tolerable than A230U. In the first case, the ligation junction is UA**U**A↓GGAA, and in the second case it is **A**A**U**A↓GGAA (mutations relative to wild-type P4-P6 in boldface). In both ligations, $R^{P4\text{-}P6}$ also contained the remaining three mutations in L6b as described above. Each ligation was performed with 0.6 nmol $L^{P4\text{-}P6}$, 0.8 nmol E, and 1.0 nmol $R^{P4\text{-}P6}$, to ensure that each molecule of $L^{P4\text{-}P6}$ was saturated with its binding partners and thus had optimal chance to ligate. Ligation reactions were each performed in 60 µl total volume with 40 mM Mg^{2+} for 12 h. The crude products were ethanol-precipitated and purified by 6% PAGE, for which a UV-shadowing image is shown in Figure X9. The reaction in which the substrates were joined at the UAUA↓GGAA junction afforded 33% yield of ligated P4-P6, while the AAUA↓GGAA ligation provided about 7% yield, which represented sufficient material for several radiolabelings. These results are quantitatively consistent with the yields after 12 h that were expected based on the smaller-scale reactions described earlier. Both of the ligated P4-P6 derivatives were then assayed structurally by nondenaturing gel electrophoresis.

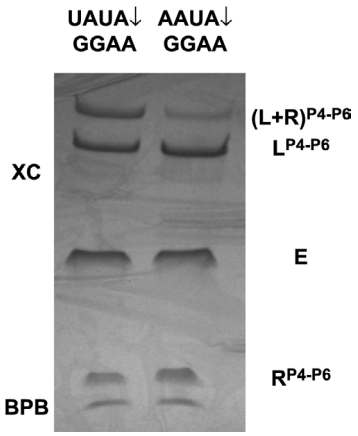

Figure X9. Preparative ligation reactions with the 9A6 deoxyribozyme to form P4-P6. The four RNA nucleotides on each side of the A233↓G234 ligation junction are shown above each lane of the 6% PAGE image, visualized by UV shadowing on a fluorescent TLC plate. The identities of the nucleic acid species are shown on the right side; the positions of the dyes xylene cyanol (XC) and bromophenol blue (BPB) are labeled on the left.

Nondenaturing gel electrophoresis assays of Mg^{2+}-dependent P4-P6 folding

The two P4-P6 derivatives prepared by deoxyribozyme-mediated ligation (Figure X9) were radiolabeled (γ-^{32}P-ATP, T4 polynucleotide kinase) and assayed for Mg^{2+}-dependent folding by nondenaturing (native) polyacrylamide gel electrophoresis in 1× TB (Tris-borate) buffer at 35 °C, using methods described previously (ref. 1). P4-P6 derivatives of the same sequences but with all 3'–5' linkages were prepared by in vitro transcription from PCR-derived DNA templates, radiolabeled, and electrophoresed in the same gels for comparison. Representative native gel images are shown in Figure X10A. From the shifts in the mobility vs. [Mg^{2+}] curves of Figure X10B, the free energy perturbation $\Delta\Delta G°'$ due to the changes in sequence and/or phosphodiester linkage were calculated. For the AAUA↓GGAA ligation product, the $\Delta\Delta G°'$ for both the 3'–5' linked P4-P6 (mut3') and the 2'–5' linked P4-P6 (mut2') were <0.2 kcal/mol. These values are extremely small and indicate that neither the nucleotide changes necessary to enable ligation nor the 2'–5' linkage created by the deoxyribozyme interfere significantly with the Mg^{2+}-dependent P4-P6 structure. For the UAUA↓GGAA ligation product, the $\Delta\Delta G°'$ values were nonzero but still rather small: 0.5 ± 0.3 kcal/mol (mut3') and 0.7 ± 0.3 kcal/mol (mut2'). Thus the U-U mismatch introduced into the stem does introduce a measurable thermodynamic perturbation. Nevertheless, at high [Mg^{2+}] the ligated RNA migrates equivalently to wild-type P4-P6, suggesting that the fully folded structure of the mutant RNA is similar to that of the wild-type RNA. Significantly, for both ligated products there is almost no difference between the folding of mut3' and mut2' at any [Mg^{2+}]. This indicates that the presence of a 2'–5' linkage rather than 3'–5' linkage between A233 and G234 (independent of the base changes) matters very little for P4-P6 folding.

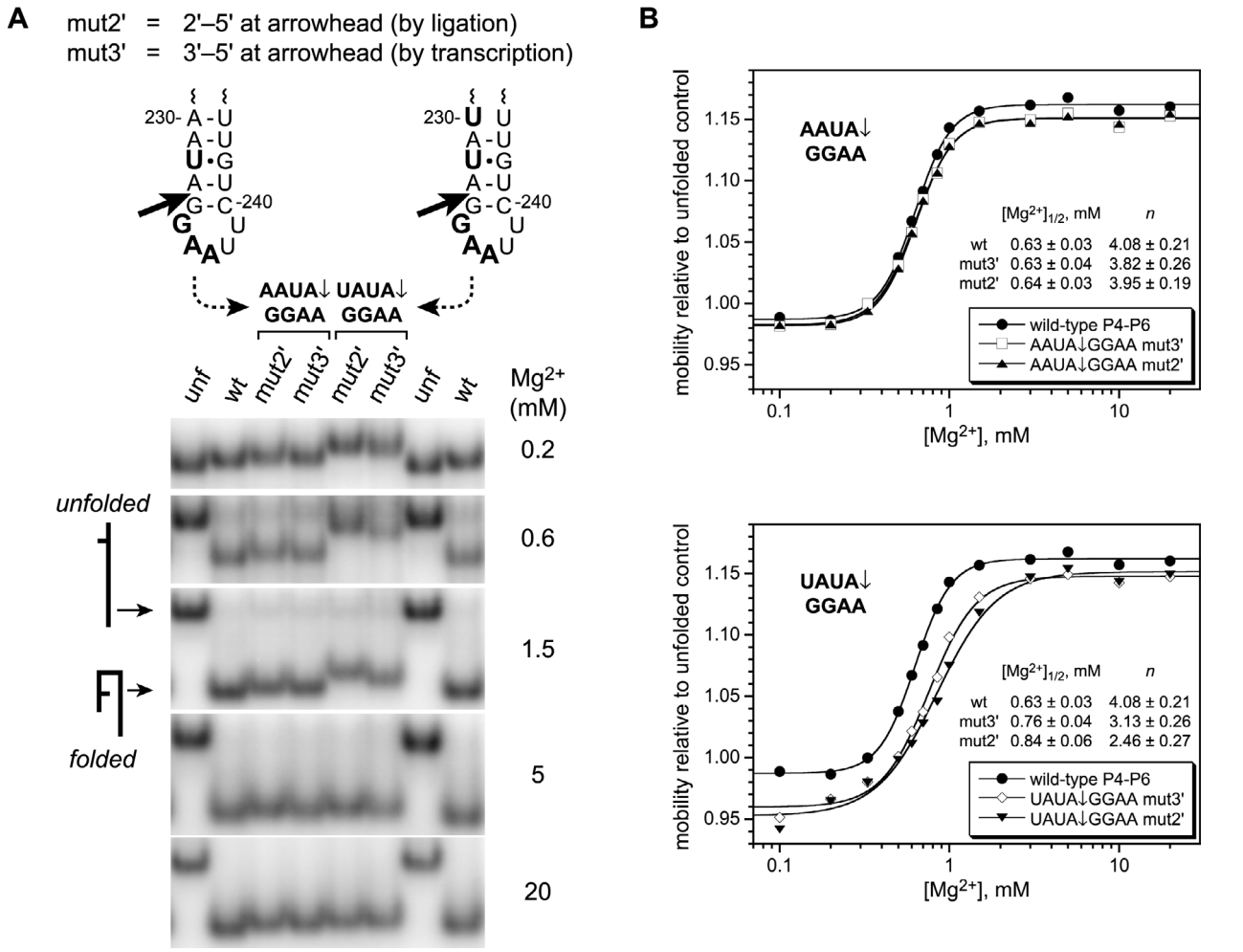

Figure X10. Nondenaturing gel electrophoresis demonstrates that P4-P6 prepared by deoxyribozyme-mediated ligation folds like wild-type P4-P6 in the presence of Mg^{2+}. (A) Representative gel images obtained at various Mg^{2+} concentrations (1× TB, 35 °C). Samples: wt, wild-type P4-P6 RNA; unf, unfolded control mutant (see ref. 1); mut3', mutant P4-P6 with a 3'–5' A233↓G234 ligation junction prepared by in vitro transcription; mut2', mutant P4-P6 with a 2'–5' A233↓G234 ligation junction prepared by deoxyribozyme-mediated ligation. The RNA nucleotides immediately surrounding the ligation junction are shown. (B) Plots of mobility versus $[Mg^{2+}]$, fit as described in ref. 1. The $[Mg^{2+}]_{1/2}$ values and Hill coefficients *n* are shown on the plots.